ELSEVIER

Journal of Organometallic Chemistry 565 (1998) 271–277

Journal of Organometallic Chemistry

Organometallic clusters: What is an appropriate DFT treatment?[1]

Michael J. Liddell *

Department of Chemistry, James Cook University, Cairns Campus, Cairns, Qld, Australia

Received 13 January 1998

Abstract

This communication looks at the accuracy of various non-local density functional theory (NL-DFT) methods in computing the geometries and relative energies of $Mn_2(CO)_{10}$ (**1**) and three iron carbonyl clusters, $Fe_3(\mu_3\text{-}\eta^2\text{-}HC_2H\text{-}//)(\mu\text{-}CO)(CO)_9$ (**2**), $Fe_3(\mu_3\text{-}\eta^2\text{-}C_2H_2)(\mu\text{-}CO)(CO)_9$ (**3**), and $Fe_3(\mu_3\text{-}\eta^2\text{-}HC_2H\text{-}\perp)(CO)_9$ (**4**). The Becke–Perdew non-local functional (BP86) is found to outperform the hybrid B3LYP functional, in particular when used with numeric orbital basis sets.

Keywords: Density functional theory; Iron; Clusters; Manganese; Alkyne; Vinylidene

1. Introduction

The most appropriate theoretical method for studying the electronic properties of small organometallic clusters is currently not well defined. Clearly with the great activity in non-local density functional theory (NL-DFT) methods [1] and the body of reported data from the study of various mononuclear organometallic systems [2], this is the most promising approach to look at. This communication looks at the performance of two of the most commonly used density functionals (BP86 [3] and B3LYP [4]) and explores the orbital basis sets that may be used reliably with them. The choice of NL-DFT[2] as an appropriate theoretical framework to describe clusters is one based on practicality. A sophisticated treatment of electron correlation has been shown to be important for most transition metal systems [5]. The multiconfigurational methods CASSCF and CASPT2 [6] are correct for these systems but suffer from program limitations, as they cannot correlate the large number of electrons found in polymetallic systems. Other higher level correlation treatments such as QCISD(T) and CCSD(T) [7] also give accurate geometries and energies for organometallic systems but suffer from the same problem in that there are simply too many electrons to correlate. These higher level methods are useful as benchmarks and recently an evaluation of CASPT2 and NL-DFT methods for studying mononuclear nickel olefin compounds [8] has demonstrated that the optimized geometries and relative energies of stationary points are of comparable accuracy with both techniques.

Rösch and Pacchioni have published several papers [9] on the electronic structure of a series of nickel carbonyl clusters (Ni_n $n = 5$–44) using the X_α DFT approximation. Holland et al. [10] also used the X_α approximation in a study of several M_4 carbonyl clusters (M = Fe, Co, Ni), as did Furet et al. [11] for $Ni_8(\mu_4\text{-}PPh)_6(CO)_8$ and related clusters. Although a low level DFT approximation, the X_α results were sufficiently accurate to provide preliminary interpretation of optical spectra and paved the way for the increased activity in DFT methods. A recent paper on the elec-

* Tel.: +61 740 421275; e-mail: michael.liddel@jcu.edu.au

[1] Dedicated to Professor Michael Bruce, an inspirational cluster chemist, on the occasion of his 60th birthday.

[2] NL-DFT is used here to include non-local gradient corrected functionals such as BP86 and hybrid functionals such a B3LYP which include some amount of pure Hartree–Fock exchange.

0022-328X/98/$19.00
PII S0022-328X(98)00624-X

Table 1
Internal basis sets used for NL-DFT calculations on compounds (**1**)–(**5**)

Code	Internal name	Basis set description[a]
I	G94 LanL2DZ	Hay–Wadt pseudopotential and DZ basis set (Mn, Fe); Dunning DZ (C,O,H)
II	G94 6–311; D95	Wachters TZ basis set (metal); Dunning DZ (C,O,H)
III	G94 6–311+; D95	II+diffuse functions 1s,2p,1d (metal)
IV	G94 6–311; D95*	II+1 d polarization function (C,O)
V	G94 6–311+G*	III+1f polarization function (Mn); TZ+diffuse+polarization (C,O)
VI	S5.0 DN*	Double numeric with polarization functions. TZ (metal); DZP (C,O,H)

[a] G94, Gaussian 94; S5.0, Spartan5.0; DZ, double zeta; TZ, triple zeta; P, polarization.

tronic structure of $[M_{10}(\mu_6\text{-C})(CO)_{24}]^{2-}$ clusters (M = Ru, Os) [12] used the LSD functional at an idealized geometry, as did earlier work by Bullett [13] on a series of osmium carbonyls. The basic LSD functional provides substantially improved molecular energies when compared with the X_α approximation and these two studies demonstrated the utility of this functional in the analysis of UV-Visible and photoelectron spectra of carbonyl clusters. More recently the non-local BLYP functional has been used by Dance [14] in studies on metallocarbohedrenes and similar systems have also been looked at with the BP86 functional [15]. A large body of DFT work on organometallic and transition metal cluster systems has been published by the groups of Ziegler [2,16], Baerends [17,18] and Salahub [19] who have recently been using non-local gradient corrected functionals such as BP86. The variety of systems that have been investigated and the extensive comparison with experimental data has established that these non-local functionals give a substantially better treatment of organometallic systems than LSD and, in an overall sense, this is an accurate and reliable level of theory to use. There is also a significant amount of work on organometallic systems, in particular smaller ones, where the B3LYP functional has performed well [20–26]. In a recent paper [27] it was established that the BP86 functional provided reaction enthalpies for a set of small main group systems that were in better agreement with experiment than the B3LYP functional. It was therefore of interest to compare the performance of these two functionals with some reasonably large metal–metal bonded organometallic systems.

Table 2
$Mn_2(CO)_{10}$ (**1**) D_{4d} conformer

	B3LYP/I	B3LYP/V	BP86/I	BP86/II	BP86/IV	BP86/V	BP86/VI[b]	BP86/ADF	X-ray[a]
Mn–Mn	2.972	3.034	2.925	3.004	2.956	2.978	3.004	3.034	2.895(1)
$Mn–C_{equatorial}$	1.848	1.871	1.835	1.834	1.842	1.856	1.858	1.871	1.859(3)
$Mn–C_{axial}$	1.798	1.819	1.788	1.787	1.794	1.806	1.813	1.822	1.820(3)
$C–O_{equatorial}$	1.174	1.141	1.188	1.190	1.168	1.155	1.157	1.155	1.140(4)
$C–O_{axial}$	1.175	1.143	1.190	1.193	1.172	1.158	1.160	1.158	1.150(4)

Comparison of selected computed distances (Å).
[a] (av) Averaged over equivalent interatomic distances.
[b] Due to program limitations the Spartan calculation was carried out in D_2 symmetry with literature values from the 74K X-ray diffraction study [31] and ADF study [17]c.

Table 3
$Fe_3(\mu_3\text{-}\eta^2\text{-}HC_2H\text{-}//)(\mu\text{-CO})(CO)_9$ (**2**)

	B3LYP/I	B3LYP/II	B3LYP/IV	BP86/I	BP86/II	BP86/III	BP86/IV	BP86/VI	X-ray[a36]
$Fe_1–Fe_2$	2.567	2.593	2.577	2.557	2.579	2.575	2.563	2.579	2.534(1)
$Fe_2–Fe_3$	2.706	2.729	2.713	2.664	2.681	2.679	2.664	2.680	2.665(1)
$Fe_1–C_1$	2.119	2.094	2.076	2.105	2.081	2.091	2.063	2.077	2.073(3)
Fe–C(O) (av)	1.792	1.782	1.791	1.780	1.774	1.786	1.781	1.799	1.810(4)
$Fe_2–C_1$	1.979	1.969	1.963	1.982	1.971	1.981	1.965	1.993	1.980(3)
$C_1–C_2$	1.396	1.398	1.388	1.404	1.407	1.405	1.396	1.384	1.394(6)
Fe-μ-C(O)	2.021	2.009	2.017	2.008	1.996	2.005	2.001	2.021	2.020(4)
C–O (av)	1.174	1.175	1.155	1.189	1.191	1.190	1.170	1.158	1.137(4)
C–O (μ-)	1.191	1.194	1.171	1.206	1.209	1.208	1.185	1.174	1.153(6)

Comparison of selected computed distances (Å) with literature values for $Fe_3[\mu_3\text{-}\eta^2\text{-}(MeOCH_2)C_2(CH_2OMe)\text{-}//](\mu\text{-CO})(CO)_9$ [36].
[a] (av) Averaged over equivalent interatomic distances.

Table 4
$Fe_3(\mu_3\text{-}\eta^2\text{-}C_2H_2)(\mu\text{-}CO)(CO)_9$ (**3**)

	B3LYP/I	B3LYP/II	B3LYP/IV	BP86/I	BP86/II	BP86/III	BP86/IV	BP86/VI	X-ray[a37]
$Fe_1–Fe_2$	2.593	2.617	2.601	2.594	2.622	2.624	2.603	2.624	2.603(1)
$Fe_2–Fe_3$	2.592	2.591	2.581	2.567	2.569	2.575	2.556	2.567	2.547(1)
$Fe_1–C_1$	2.036	2.022	2.005	2.032	2.025	2.026	2.010	2.010	1.966(6)
$Fe_1–C_2$	2.288	2.238	2.204	2.280	2.235	2.239	2.199	2.241	2.194(6)
Fe–C(O) (av)	1.791	1.782	1.792	1.779	1.773	1.787	1.781	1.799	1.812(9)
$Fe_2–C_1$	1.913	1.899	1.894	1.915	1.901	1.907	1.895	1.918	1.889(6)
$C_1–C_2$	1.393	1.398	1.391	1.404	1.407	1.408	1.400	1.389	1.399(9)
$Fe–\mu$-C(O)	2.013	1.992	2.000	2.002	1.982	1.991	1.988	2.014	2.018(7)
C–O(av)	1.174	1.175	1.155	1.189	1.191	1.191	1.170	1.158	1.13(1)
C–O ($\mu-$)	1.188	1.190	1.168	1.204	1.207	1.207	1.183	1.173	1.147(7)

Comparison of selected computed distances (Å) with literature values for $Fe_3[\mu_3\text{-}\eta^2\text{-}C_2H_2](\mu\text{-}CO)(CO)_9$ [37].
[a] (av) Averaged over equivalent interatomic distances.

Table 5
$Fe_3(\mu_3\text{-}\eta^2\text{-}HC_2H\text{-}\perp)(CO)_9$ (**4**)

	B3LYP/I	B3LYP/II	B3LYP/IV	BP86/I	BP86/II	BP86/III	BP86/IV	BP86/VI	X-ray[a33]
$Fe_1–Fe_2$	2.510	2.545	2.528	2.501	2.527	2.521	2.511	2.530	2.491(10)
$Fe_2–Fe_3$	2.666	2.720	2.690	2.629	2.661	2.645	2.635	2.646	2.579(11)
$Fe_1–C_2$	2.021	1.998	1.992	2.039	2.021	2.040	2.014	2.028	2.048(16)
Fe–C(O) (av)	1.784	1.773	1.782	1.771	1.764	1.775	1.771	1.789	1.755(24)
$Fe_2–C_1$	1.957	1.920	1.910	1.958	1.923	1.948	1.913	1.941	1.946(16)
$Fe_2–C_2$	2.124	2.098	2.079	2.082	2.050	2.061	2.034	2.048	2.071(16)
$C_1–C_2$	1.409	1.428	1.413	1.426	1.445	1.432	1.430	1.406	1.409(22)
C–O (av)	1.175	1.176	1.156	1.190	1.192	1.192	1.171	1.159	1.159(24)

Comparison of selected computed distances (Å) with literature values for $Fe_3(\mu_3\text{-}\eta^2\text{-}PhC_2Ph\text{-}\perp)(CO)_9$ [33].
[a] (av) Averaged over equivalent interatomic distances.

2. Computational methods

Calculations have been carried out using Gaussian94 [28] and Spartan5.0 [29] on either Silicon Graphics Power Challenge/R8000 or IBM SP2 computers. Clusters were optimized within C_s symmetry and the other molecules within the stated symmetry. The internal orbital basis sets which were used are detailed in Table 1. Emphasis is placed on the differences between calculated interatomic distances and the corresponding experimental values in Tables 2–6. In general, such distances are a good indicator of the quality of the computed geometry and thus the analysis of these quite large systems has been simplified considerably. Due to the size of the systems, frequency calculations verifying the true nature of the optimized minima were carried out only in selected cases.

Table 6
$Fe_3(\mu_3\text{-}\eta^2\text{-}MeC_2Me\text{-}\perp)(CO)_9$ (**5**)

	BP86/I	BP86/I*[a]	BP86/VI	X-ray[b33]
$Fe_1–Fe_2$	2.484	2.492	2.499	2.491(10)
$Fe_2–Fe_3$	2.620	2.616	2.630	2.579(11)
$Fe1–C_2$	2.076	2.059	2.088	2.048(16)
Fe–C(O) (av)	1.769	1.765	1.788	1.755(24)
$Fe_2–C_1$	1.966	1.935	1.960	1.946(16)
$Fe_2–C_2$	2.108	2.076	2.086	2.071(16)
$C_1–C_2$	1.439	1.427	1.410	1.409(22)
C–O (av)	1.191	1.170	1.161	1.159(24)

Comparison of selected computed distances (Å) with literature values for $Fe_3(\mu_3\text{-}\eta^2\text{-}PhC_2Ph\text{-}\perp)(CO)_9$ [33].
[a] Polarization functions were used from the internal G94 basis set D95* (C, O).
[b] (av) Averaged over equivalent interatomic distances.

3. Results and discussion

Several DFT theoretical studies have been carried out on $Mn_2(CO)_{10}$ (**1**) [16,17,30] and to start this investigation the performance of the various functionals and basis sets were compared with these earlier results. The density functional (BP86) results which have been reported by Ziegler [16] and by Baerends [17] for $Mn_2(CO)_{10}$, made use of the ADF program which uses Slater Type Orbital (STO) basis sets. I have used computer programs which use different implementations of NL-DFT to optimize the D_{4d} conformation of (**1**), the results are tabulated under functional/basis code (e.g.

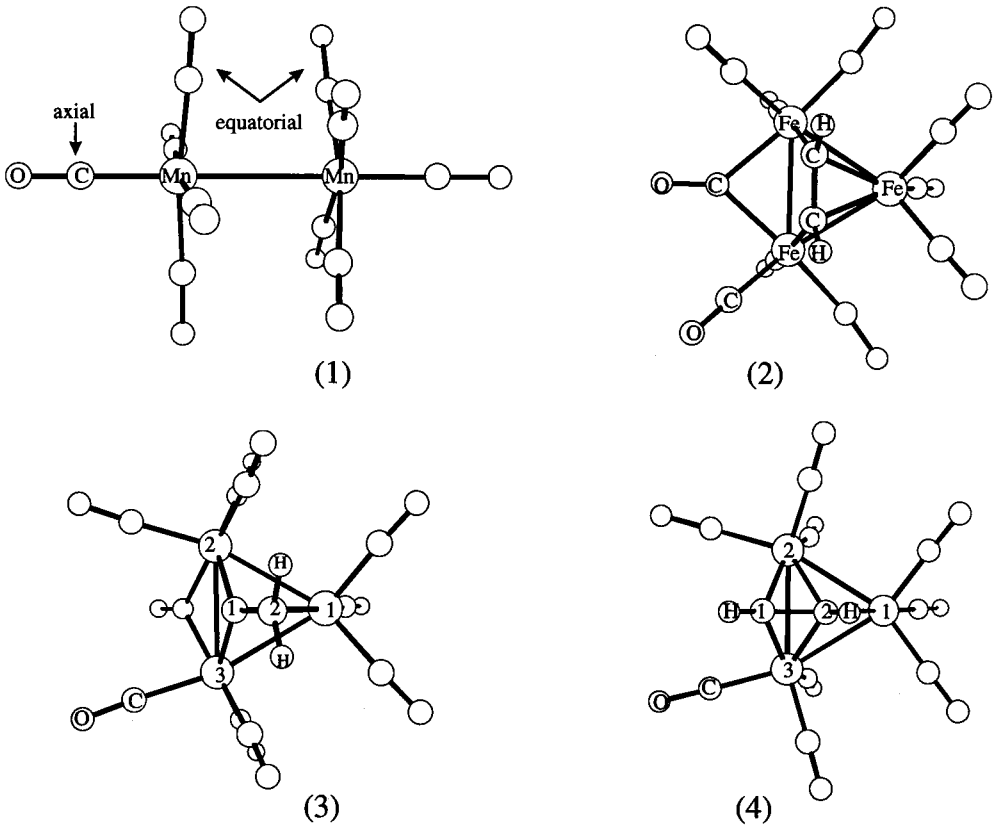

Fig. 1. BP86/VI structures of (**1**), (**2**), (**3**) and (**4**) showing the atom numbering schemes used.

Table 7
Comparison of the relative energies of the clusters (**2**), (**3**) and {(**4**)+CO} (kcal mol^{-1})

Cluster	B3LYP/I	B3LYP/II	B3LYP/IV	BP86/I	BP86/II	BP86/IV	BP86/II// BP86/VI[a]	BP86/VI// BP86/II	BP86/VI
(**2**)	12.2	11.5	10.9	11.8	11.4	10.8	11.2	11.9	9.2
(**3**)	0	0	0	0	0	0	0	0	0
(**4**)+CO	32.3	28.7	25.5	37.7	34.6	31.4	35.0	25.6	21.7

[a] BP86/II // BP86/VI means BP86/II energies were calculated at BP86/VI geometries.

BP86/IV) in Table 2. The data for basis sets I–V were obtained with Gaussian94 which uses a Gaussian Type Orbital (GTO) basis set while those for basis set VI were obtained with Spartan5.0 using a Numerical Type Orbital (NTO) basis set. With the relatively small basis set II the BP86 functional provided results within 0.05 Å of Baerends ADF result [17]c (where the basis set was effectively saturated), extension of the GTO basis set to BP86/IV and then BP86/V established that the good agreement for BP86/II was fortuitous. Use of the numerical basis set VI provided results of comparable accuracy to the best GTO values (BP86/V). The B3LYP optimizations produced a Mn–Mn distance around 0.05 Å longer than the BP86 results for both the basis sets looked at [I (DZ, pseudopotential), V (TZ*+, all electron)], a similar trend was found for the Mn–C distances while the C–O distances were smaller and closer to the experimental results with the B3LYP functional. All methods appear to describe the geometry reasonably well with a converged Mn–Mn distance of 3.00 ($\pm$0.03 Å) indicated for the BP86 functional. The B3LYP functional does not improve the computed metal–metal distance, which with the large basis set V is 0.13 Å larger than the X-ray value [31] (2.895 Å). Both the DFT functionals therefore give computed Mn–Mn distances which are longer than the X-ray result by at least 0.1 Å indicating that there is room for improvement in the underlying functionals. Recently, there has been some controversy over the energy difference between the D_{4d} and D_{4h} conformers of $Mn_2(CO)_{10}$ [30]. Using the BP86/V and B3LYP/V methods the difference is 4.6 and 4.5 kcal mol^{-1}, while with the BP86/VI method the D_{4d} staggered conformer is found to be only 1.5 kcal mol^{-1} below the D_{4h}

eclipsed conformer, suggesting that a more accurate method such as CCSD(T) is necessary to accurately calibrate the energetic separation.

The series of clusters that has been investigated comprises $Fe_3(\mu_3\text{-}\eta^2\text{-}HC_2H\text{-}//)(\mu\text{-}CO)(CO)_9$ (**2**), $Fe_3(\mu_3\text{-}\eta^2\text{-}C_2H_2)(\mu\text{-}CO)(CO)_9$ (**3**), $Fe_3(\mu_3\text{-}\eta^2\text{-}HC_2H\text{-}\perp)(CO)_9$ (**4**) and $Fe_3(\mu_3\text{-}\eta^2\text{-}MeC_2Me\text{-}\perp)(CO)_9$ (**5**); optimized structures of (**2**), (**3**) and (**4**) are illustrated in Fig. 1. The first two clusters are structural isomers in respect to the acetylene derived ligand: (**2**) an alkyne ligand and (**3**) a vinylidene ligand. Cluster (**4**) is related to (**2**) by the loss of the bridging carbonyl ligand and the reorientation of the alkyne which has changed from a parallel to a perpendicular orientation. Cluster (**5**), which is the 2-butyne analogue of (**4**), was looked at to estimate the effect of the alkyne substituents on the interatomic parameters that were being studied. Previous molecular orbital studies on clusters such as (**4**) have focused on rationalizing the observed bonding patterns at a qualitative level using Extended Hückel theory [32]. In Tables 3–6 are listed the results from the optimization of clusters (**2**)–(**5**) using various DFT/basis set combinations and for comparison the X-ray results reported for related clusters. The trends follow those established with $Mn_2(CO)_{10}$, the B3LYP functional in general provides poorer agreement with experiment in the metal–metal distances when compared with the BP86 functional across the basis sets looked at (I, II and IV). The B3LYP Fe–Fe distances are generally larger than the X-ray values (-0.002–0.140 Å) and range from -0.005 to $+0.059$ Å larger than the BP86 results. As found for $Mn_2(CO)_{10}$ the C–O distances are described better by the B3LYP functional but the discrepancy with experiment is still substantial for clusters (**2**) and (**3**) (>0.015 Å).

The standard deviations in the reported X-ray Fe–Fe distances are useful when making comparisons with the computed results, and in a few instances agreement is achieved. The deviations in the measured Fe–C and C–O distances are, however, of little use due to the considerable variation in apparently symmetry equivalent distances. This is not a peculiarity of the clusters as $Mn_2(CO)_{10}$ shows variations for the equatorial Mn–C distances of 1.850(3)–1.867(3) Å in the accurate 74K X-ray determination [31]. The best performing method I have therefore judged as the one where there are fewest calculated distances which deviate by more than 0.03 Å from the X-ray results for the Fe–Fe and Fe–C distances and 0.02 Å for the C–O distances. Until such calculations provide an overall level of accuracy in the key structural parameters of <0.02 Å, a more detailed break down (such as individual carbonyl distances, angles, torsions and overall RMS deviations) is not justified. Using the above criterion, the BP86/VI approach is the most successful for clusters of this size, closely followed by B3LYP/IV. In general the addition of polarization functions improves the carbonyl distances as is seen in the differences between the basis set II and IV results where the average C–O distance decreased by 0.02 Å towards the X-ray values when polarization functions were added. The B3LYP method as expected gives C–O distances which are closer to experiment than the BP86 method within a given basis set. The BP86/VI method performs at a similar level of accuracy to the B3LYP/IV method in the C–O distances and it would seem the numeric basis set VI is more complete than the equivalent gaussian basis set IV. As noted by others [8] the LanL2DZ pseudopotential plus valence basis set (I) performs surprisingly well on many occasions. In this case, for cluster (**5**), the results obtained with basis set I (to which main group polarization functions had been added) were in closest agreement with the X-ray structure of $Fe_3(\mu_3\text{-}\eta^2\text{-}PhC_2Ph\text{-}\perp)(CO)_9$ [33]. Changing from proton (**4**) to methyl substituents (**5**) on the alkyne of the model cluster gave minor improvements in the calculated Fe–Fe distances (0.01 Å) which, in conjunction with polarized basis sets, gave the closest agreement with experiment.

Another criterion of the success of the selected methods is in the computed energetic differences between the clusters. As shown in Table 7, all methods predict a difference in energy of -10 (± 3) kcal mol^{-1} between the structural isomers (**2**) and (**3**), with the vinylidene cluster being the most stable. This contrasts with the vinylidene-acetylene isomerization reaction of free 'HC_2H' where acetylene is placed at significantly lower energy than vinylidene at the MP4 level (-46 kcal mol^{-1}) [34] and at the BP86/VI level (-44 kcal mol^{-1}). Not only has the interaction of the vinylidene ligand with the cluster made this ligand a stable entity, but it has also made it the most stable isomeric form of the 'HC_2H' ligand in this cluster system. Larger differences between the computational methods are seen in the energy change accompanying the transformation from (**3**) to (**4**), which involves the breaking of two Fe–CO bonds and the loss of the bridging carbonyl ligand. The difference between the B3LYP and BP86 calculations within a given basis set are at the level of $+6$ kcal mol^{-1} and the change from basis set I–IV alters the energy by around -6 kcal mol^{-1}. A significant variation is seen in the reaction energetics predicted by the BP86/II and BP86/VI methods which are -13 kcal mol^{-1} apart. Calculation of the energies at the BP86/II geometries using the BP86/VI method and conversely at the BP86/VI geometries with the BP86/II method demonstrated that there are significant differences between the two basis sets. Of the two methods the more reliable is BP86/VI as shown by including BP86/IV in

the comparison where the GTO basis set had been extended to include polarization functions on carbon and oxygen, the extension of the GTO basis set is seen to move the values closer to the NTO (BP86/VI) results. To provide a more quantitative basis for this assertion the so-called 'bond snapping' energies (i.e. no geometric relaxation of the products) were calculated for $Cr(CO)_6$ and $Mn_2(CO)_{10}$ using the BP86/II and BP86/VI methods. These bond snapping energies have been reported previously by Rosa et al. [17]c and, given a reasonable (i.e. low basis set superposition error) basis set, values of 45 (± 1) and 29 (± 1) kcal mol^{-1} should be obtained for $Cr(CO)_6 \rightarrow Cr(CO)_5 + CO$ and $Mn_2(CO)_{10} \rightarrow 2 \times Mn(CO)_5^{\bullet}$, respectively. The values obtained with BP86/VI (44, 29 kcal mol^{-1}) and BP86/II (50, 31 kcal mol^{-1}), indicate that of the two methods, BP86/VI gives closest agreement with the saturated basis set ADF calculations and by extension good agreement with experiment.

4. Conclusions

The comparison between the performance of the BP86 and B3LYP functionals in several multi-metallic systems has indicated that the BP86 method describes the internuclear metal–metal separation more successfully than the hybrid B3LYP method. The development of NL-DFT functionals has relied extensively on calibration with atomic and organic systems which obviously does not lead to optimal functionals for systems with transition metal bonds as shown by the overestimated Mn–Mn separation for $Mn_2(CO)_{10}$. This is not to say that the functionals provide results of low accuracy, but rather the results are not as accurate as that typically found for the B3LYP method with organic systems [35]. For the clusters studied, the most reliable method was BP86/VI where the computed Fe–Fe and Fe–C distances were at worst 0.06 Å and the C–O distances at worst 0.03 Å away from the related X–ray results. The closest approach to experiment in the computed interatomic distances is obtained when complex acetylene ligands are modeled with 2-butyne rather than acetylene. Extension of the basis set has demonstrated that for geometry optimization it is better to include polarization functions on the main group atom basis set than to place diffuse functions on the metal basis, for comparative energetics it is essential that these polarization functions are included and also the metal basis must be of triple zeta quality. Further work is in progress on the utility of these methods for heterometallic cluster systems and in the comparison of the BP86 functional with high-level ab-initio methods using simple cluster systems.

Acknowledgements

This work was enabled by the support of the James Cook University Research Office. Computing resources and the helpful assistance provided by staff at the High Performance Computing Centre (James Cook University) and the Queensland Parallel Supercomputing Facility (Griffith University) are also acknowledged.

References

[1] J.M. Seminario, P. Politzer (Eds.), Modern Density Functional Theory: A Tool for Chemistry, Elsevier, Amsterdam, 1995.
[2] T. Ziegler, Chem. Rev. 91 (1991) 651; T. Ziegler, Can. J. Chem. 73 (1995) 743; H. Jacobsen, T. Ziegler, J. Am. Chem. Soc. 118 (1996) 4631.
[3] A.D. Becke, Phys. Rev. A 38 (1988) 3098; J.P. Perdew, Phys. Rev. B 33 (1986) 8822.
[4] P.J. Stephens, F.J. Devlin, C.F. Chabalowki, M.J. Frisch. J. Phys. Chem. 98 (1994) 11623; A.D. Becke, J. Chem. Phys. 98 (1993) 5648; C. Lee, W. Yang, R.G. Parr, Phys. Rev. B 37 (1988) 785.
[5] P.E.M. Siegbahn, Adv. Chem. Phys. 93 (1996) 333.
[6] B.O. Roos, P.R. Taylor, P.E.M. Siegbahn, Chem. Phys. 48 (1980) 157; K. Andersson, P.-A. Malmqvist, B.O. Roos, J. Chem. Phys. 96 (1992) 1218.
[7] J. A. Pople, M. Head-Gordon, K. Raghavachari, J. Chem. Phys. 87 (1987) 5968.
[8] F. Bernardi, A. Bottoni, M. Calcinari, I. Rossi, M.A. Robb, J. Phys. Chem. A 101 (1997) 6310.
[9] G. Pacchioni, N. Rösch, Acc. Chem. Res. 28 (1995) 390; N. Rösch, L. Ackermann, G. Pacchioni, B.I. Dunlap, J. Chem. Phys. 95 (1991) 7004; G. Pacchioni, N. Rösch, Inorg. Chem. 29 (1990) 2901; N. Rösch, L. Ackermann, G. Pacchioni, J. Am. Chem. Soc. 114 (1992) 3549.
[10] G.F. Holland, D.E. Ellis, W.C. Trogler, J. Chem. Phys. 83 (1985) 3507.
[11] E. Furet, A. Le Beuze, J.-F. Halet, J.-Y. Saillard, J. Am. Chem. Soc. 116 (1994) 274.
[12] M.P. Cifuentes, M.G. Humphrey, J.E. McGrady, P.J. Smith, R. Stranger, K.S. Murray, B. Moubaraki, J. Am. Chem. Soc. 119 (1997) 2647.
[13] D.W. Bullett, Chem. Phys. Lett. 135 (1987) 373.
[14] I. Dance, J. Am. Chem. Soc. 118 (1996) 6309.
[15] J. Munoz, J.C. Pujol, C. Bo, J.-M. Poblet, M.-M. Rohmer, M. Benard, J. Phys. Chem. A. 101 (1997) 8345.
[16] E. Folga, T. Ziegler, J. Am. Chem. Soc. 115 (1993) 5169.
[17] A. Rosa, G. Ricciardi, E.J. Baerends, D.J. Stufkens, Inorg. Chem. 34 (1995) 3425; (b) A. Rosa, G. Ricciardi, E.J. Baerends, D.J. Stufkens, Inorg. Chem. 35 (1996) 2886; (c) A. Rosa, A.W. Ehlers, E.J. Baerends, J.G. Snijders, G. te Velde, J. Phys. Chem. 100 (1996) 5690.
[18] P. Belanzoni, M. Rosi, A. Sgamellotti, E.J. Baerends, C. Floriani, Chem. Phys. Lett., 257 (1996) 41; P. Belanzoni, N. Re, M. Rosi, A. Sgamellotti, E.J. Baerends, C. Floriani, Inorg. Chem., 35 (1996) 7776; A. Rosa, G. Ricciardi, E.J. Baerends, D.J. Stufkens, J. Phys. Chem. 100 (1996) 15346; M.P. Wilms, E.J. Baerends, A. Rosa, D.J. Stufkens, Inorg. Chem., 36 (1997) 1541.
[19] A. Rochefort, J. Andzelm, N. Russo, D.R. Salahub, J. Am. Chem. Soc. 112 (1990) 8239; M. Castro, D.R. Salahub, Phys. Rev. B 49 (1994) 11842; C. Jamorski, A. Martinez, M. Castro, D.R. Salahub, Phys. Rev. B 55 (1997) 10905.

[20] M. Stahl, U. Pidun, G. Frenking, Angew. Chem. Int. Ed. Engl. 36 (1997) 2234.
[21] K. Spears, J. Phys. Chem. A 101 (1997) 6273.
[22] A. Ricca, C.W. Bauschlicher, J. Phys. Chem. 98 (1994) 12899; A. Ricca, C.W. Bauschlicher, Chem. Phys. Lett. 245 (1995) 150; A. Ricca, C.W. Bauschlicher, Theor. Chim. Acta 92 (1995) 123.
[23] C. Adamo, F. Lelj, J. Chem. Phys. 103 (1995) 10605; V. Barone, Chem. Phys. Lett. 233 (1995) 129.
[24] M.N. Glukhovtsev, R.D. Bach, C.J. Nagel, J. Phys. Chem. A 101 (1997) 316.
[25] M.C. Holthausen, A. Fiedler, H. Schwarz, W. Koch, J. Phys. Chem. 100 (1996) 6236.
[26] Q. Cui, D. G. Musaev, K. Morokuma, Organometallics 16 (1997) 1355.
[27] J.M. Martell, J.D. Goddard, L.A. Eriksson, J. Phys. Chem. A 101 (1997) 1927.
[28] Gaussian 94 (Revision B.3 or D.1), M.J. Frisch, G.W. Trucks, H.B. Schlegel, P.M.W. Gill, B.G. Johnson, M.A. Robb, J.R. Cheeseman, T.A. Keith, G.A. Petersson, J.A. Montgomery, K. Raghavachari, M.A. Al-Laham, V.G. Zakrzewski, J.V. Ortiz, J.B. Foresman, C.Y. Peng, P.Y. Ayala, M.W. Wong, J.L. Andres, E.S. Replogle, R. Gomperts, R.L. Martin, D.J. Fox, J.S. Binkley, D.J. Defrees, J. Baker, J.P. Stewart, M. Head-Gordon, C. Gonzalez, J.A. Pople, Gaussian, Inc., Pittsburgh PA, 1995.
[29] Spartan 5.0.2a2. Wavefunction, Inc., Irvine, CA 92715, 1997.
[30] S.A. Decker, O. Donini, M. Klobukowski, J. Phys. Chem. A 101 (1997) 8734.
[31] M. Martin, B. Rees, A. Mitschler, Acta Crystallogr. B38 (1982) 6.
[32] J.-F. Halet, J.-Y. Saillard, R. Lissillour, M.J. McGlinchey, G. Jaouen, Inorg. Chem. 24 (1985) 218; B.E.R. Schilling, R. Hoffmann, J. Am. Chem. Soc. 101 (1979) 3456.
[33] J.F. Blount, L.F. Dahl, C. Hoogzand, W. Hübel, J. Am. Chem. Soc. 88 (1966) 292.
[34] R. Krishnan, M.J. Frisch, J.A. Pople, P.V.R. Schleyer, Chem. Phys. Lett. 79 (1981) 408.
[35] J.B. Foresman, A. Frisch, Exploring Chemistry with Electronic Structure Methods, 2nd edn, Gaussian, Pittsburgh, PA, 1996.
[36] D. Lentz, M. Reuter, Z. Anorg. Allg. Chem. 614 (1992) 121.
[37] A. Aradi, F.-W. Grevels, C. Kruger, E. Raabe, Organometallics 7 (1988) 812.